City Research Online

City, University of London Institutional Repository

Effect of abutment-backfill limit state definition on the assessment of seismic performance

Ioannis G. Mikes[1], Res. Associate, Andreas J. Kappos, Professor
Khalifa University, United Arab Emirates

Agathoklis Giaralis, Assoc. Professor
City, University of London, UK

ABSTRACT

Over the last decades, several performance-based design and assessment procedures for bridges under earthquake loading have been put forward. For assessing seismic performance, an appropriate definition of limit states is necessary. For bridges with seat-type abutments, the importance of limit states related to damage in the abutment-backfill system is often overlooked, partly due to the use of joint gaps that substantially exceed the expected design seismic displacement of the deck; nevertheless, gap closure may still occur for earthquakes stronger than the design one, with beneficial or detrimental impact on the bridge behaviour.

Here, the important limit states of 'operationality' and 'collapse prevention' are defined using different criteria for the various bridge components, including the abutment-backfill system; for the latter, displacement-based criteria that express damage in the backfill and the shear keys and their effect on the entire bridge were used for the longitudinal and the transverse direction, respectively. The effect of the selected criteria which are subject to uncertainty was studied for a typical concrete overpass. Nonlinear dynamic analyses were conducted for different levels of seismic action and the results were used to evaluate the performance of the bridge in either direction using a range of values for the criteria related to the abutment-backfill system. It was found that the abutment-backfill based limit states could be critical for certain levels of ground motion with regard to both the 'operationality' and the 'collapse prevention' of the bridge.

Keywords: Bridges, abutment, backfill, seismic assessment, limit state definition

INTRODUCTION

During the past few decades, the interest in the performance-based design and assessment of bridges has been increased since they are considered one of the most vulnerable components of road or rail networks in the case of an earthquake event, and hence critical in the assessment of the seismic risk and the resilience of these networks. As a result, various methodologies to define the limit states of concrete bridges have been proposed. Some of them utilise a single engineering demand parameter, e.g., pier ductility, to assess the performance level of the entire bridge system, while others consider the behaviour of multiple bridge components, such as piers, bearings, abutments, or foundations. Among the so-called 'component-based' methodologies, relatively few investigate the limit states of the seat-type abutment-backfill system in both the longitudinal and the transverse direction, e.g. Cardone (2014) and Stefanidou & Kappos (2017). This may be partly attributed to the limited number of experimental studies found in the literature regarding the damage states of the abutments, and partly to the fact that in many cases joint gaps larger than the design seismic deck displacement are selected by the designers. This is a common option in some seismic regions in Europe, such as Greece, to avoid the

---

[1] Corresponding Author: Ioannis Mikes, Khalifa University of Science and Technology; PhD candidate at City, University of London, UK; Ioannis.Mikes@city.ac.uk.

deck-abutment interaction and the consequent uncertainties in the estimation of the dynamic response of the bridge system in a design context.

This paper aims to investigate the effect of the definition of the abutment-backfill limit states in both directions on the assessment of bridges. Different abutment-backfill limit state thresholds are selected from the literature to account for the uncertainty inherent in their definition. To investigate the effect of accounting for abutment-related limit states and the uncertainty in their thresholds, a nonlinear model of an existing concrete overpass in Greece is subjected to a number of spectrum-compatible artificial ground motions with increasing intensity and its overall performance is assessed for both the longitudinal and the transverse direction of the bridge. The behaviour of the abutment-backfill system is simulated with nonlinear spring-gap elements described in Mikes & Kappos (2021).

METHODOLOGY

Limit state definition

Bridge fragility analysis often adopts four limit states (e.g., Cardone 2014, Stefanidou & Kappos 2017), while in the actual design of a bridge less limit states are typically considered. The limit states selected in the present work were those typically adopted for design, i.e., 'operationality' and 'collapse prevention – life safety' (LS2 and LS4). Exceedance of LS2 leads to significant damage to some elements with no risk of global or partial collapse and the need for structural repairs that affect the traffic continuity. At LS4, the structure may be able to support gravity loads but it has no sufficient margin against collapse, it is not repairable, it may be unable to withstand aftershocks, and the life safety during the earthquake event is threatened (Cardone, 2014). The corresponding 'component-based' thresholds were defined for the piers, the bearings, the foundations, and the abutment-backfill system (deck of modern bridges is not part of the seismic energy dissipation system). The selected engineering demand parameters for piers, bearings and foundation were the pier drift, the bearing deformation and the horizontal movement of footings or pile caps, respectively. The LS of the abutment-backfill system are separately defined for the longitudinal and the transverse directions, as the earthquake resistant system is quite different in each direction; in the longitudinal direction, the damage state thresholds are expressed as a function of the displacement at the top of the backwall divided by the backwall height, while in the transverse direction they are expressed as a function of the displacement of the shear keys.

The value of the limit state thresholds for piers, bearings and foundations are based on values found in the literature. Namely, the limit state threshold value of 'operationality' for the foundations is an average value of recorded permanent horizontal movements that caused serviceability interruption, adopted from Moulton (1986), while for 'collapse prevention' the seismic bearing capacity according to EN1998-5 (CEN, 2004) is adopted. It is noted that foundation rotation is not considered herein because for the specific bridge studied it remains very small even for relatively high input motion intensities (e.g., when the input motion is twice that corresponding to the design earthquake E_d, the maximum residual foundation rotation is about 10^{-3} rad). This can be attributed to the large footings and the relatively stiff foundation soil of the case-study bridge, as described in the next subsection. The LS thresholds for piers and bearings are taken from Stefanidou et al. (2022). In their database, Stefanidou et al. (2022) gathered various threshold values for different typologies of critical components recommended in the literature. These typologies match the qualitative definition of damage for the pertinent limit states, as described in Stefanidou & Kappos (2017); the same are also adopted in this work. Cylindrical piers, elastomeric bearings and surface footings were considered here, as these are used in the real bridge that served as a case study herein and is described in the next subsection. The values of these thresholds are summarised in Table 1.

Table 1. *Limit state definitions for cylindrical piers, elastomeric bearings and surface foundations*

Component	Limit state	Threshold value	Description	Reference
Pier	LS2	Drift: 1%	Concrete cracking, spalling; seismically designed pier	(Kim & Feng, 2003)
	LS4	Drift: 5%	Pier collapse; seismically designed pier	
Bearing	LS2	Shear deformation: 100%	Initiation of slipping; visible damage; yield of steel shims	(LaFave et al., 2013; Stefanidou & Kappos, 2017)
	LS4	Displacement at top: 50% of abutment seat width	Deck unseating	(Cardone, 2014)
Foundation	LS2	Horizontal movement: 38mm (1.5 inch)	Harmful but tolerable	(Moulton, 1986)
	LS4	Seismic bearing capacity	Foundation failure	(CEN, 2004)

The multiple abutment-backfill threshold values used for each limit state in either direction are shown in Table 2. To investigate the impact of the uncertainty in the definition of the abutment-backfill limit states on the assessment of the bridge, two values that roughly cover the range of the literature recommendations (excluding possible outliers) are used for each LS threshold. The values of the thresholds for the backwall-backfill system are adopted from Bozorgzadeh et al. (2008) and Stefanidou & Kappos (2017) as reported by Stefanidou et al. (2022). As for the transverse direction, two different types of damage are examined, namely damage at the shear key and significant separation between abutment and backfill; none of them is considered to control the 'collapse prevention – life safety' limit state. The damage state definition of the exterior shear keys is based on the experimental results reported by Silva et al. (2009), in a way that leads to a conservative value of LS2 threshold, whereas the case of significant separation between the abutment and the backfill is classified as LS2 by Stefanidou et al. (2022), based on the study of Xie et al. (2017). Pertinent to the case study bridge, limit states for a seat-type abutment-backfill system with granular backfill, hinging backwall (as opposed to shearing off), and shear keys monolithically connected to a strong stem wall are defined.

Table 2. *Limit state definitions for the abutment-backfill system in both directions (backwall-backfill and shear keys, respectively)*

| Component	Limit state	Threshold value	Description	Reference
Backwall-backfill (Longitudinal direction)	LS2	Displacement: $\delta(F_{max}/2)$	Stiffness reduction of the abutment-backfill system	(Bozorgzadeh et al., 2008)
		Displacement: 1% h_{bw}		(Stefanidou & Kappos, 2017)
	LS4	Displacement: $3\times\delta(F_{max})$	Ultimate deformation of abutment-backfill system	(Bozorgzadeh et al., 2008)
		Displacement: 6% h_{bw}	Ultimate deformation of abutment-backfill	(Stefanidou & Kappos, 2017)

			system (cohesionless soil)	
Abutment-Shear key-Embankment (Transverse direction)	LS2	Displacement: $\delta_{y,SK}$	Onset of yielding of the abutment-shear key reinforcement	(Silva et al., 2009)
		Displacement: 1.4% $h_{abut.}$	Significant separation between abutment and backfill	(Stefanidou et al. 2022)
	LS4	-	LS4 not controlled by abutment/shear key	-

According to the methodology adopted herein, exceedance of a limit state for at least one component as described in Tables 1 and 2 implies exceedance of the corresponding limit state of the entire bridge, based on the generally conservative assumption that the critical components of the bridge form a series system for the evaluation of its fragility (Stefanidou & Kappos, 2017). Therefore, the influence of each abutment-backfill LS definition described in Table 2 is estimated according to the effect that it had on the predicted limit state of a nonlinear bridge model subjected to a suite of spectrum-compatible accelerograms scaled to increasing intensities.

Model of the case-study bridge

Description of the studied bridge

The case-study bridge is an actual overpass of Egnatia Motorway in northern Greece (called T7) seismically designed according to modern code provisions, namely the 2000 Greek national seismic code (EAK2000) which is very similar to Eurocode 8-2 (CEN, 2005). The bridge is 99 m long, and it consists of a 45 m central span and two 27 m outer spans. The deck consists of a prestressed concrete box girder section, that is 10 m wide and has a continuously changing cross section along the bridge length (Fig. 1). The bridge has a 7% slope along its longitudinal axis. The two piers of the bridge are cylindrical with a diameter of 2 m, clear heights 5.94 m and 7.93 m each and they are monolithically connected to the deck (Fig. 2).
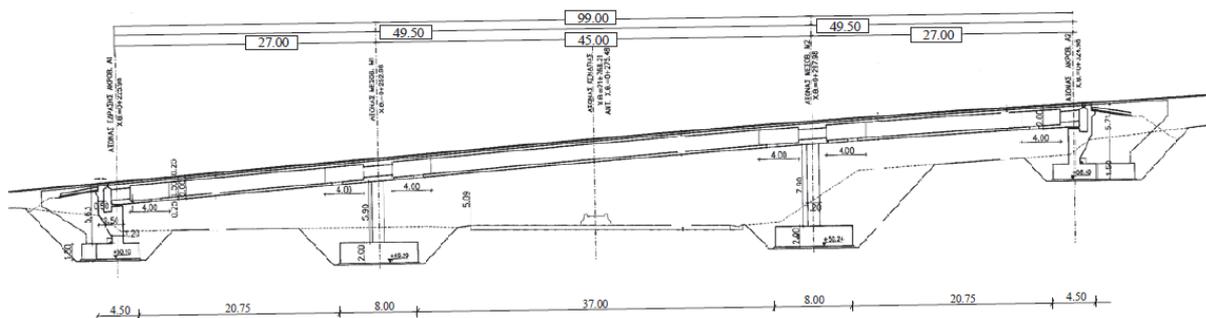

***Figure 1.** Longitudinal section of T7 bridge*
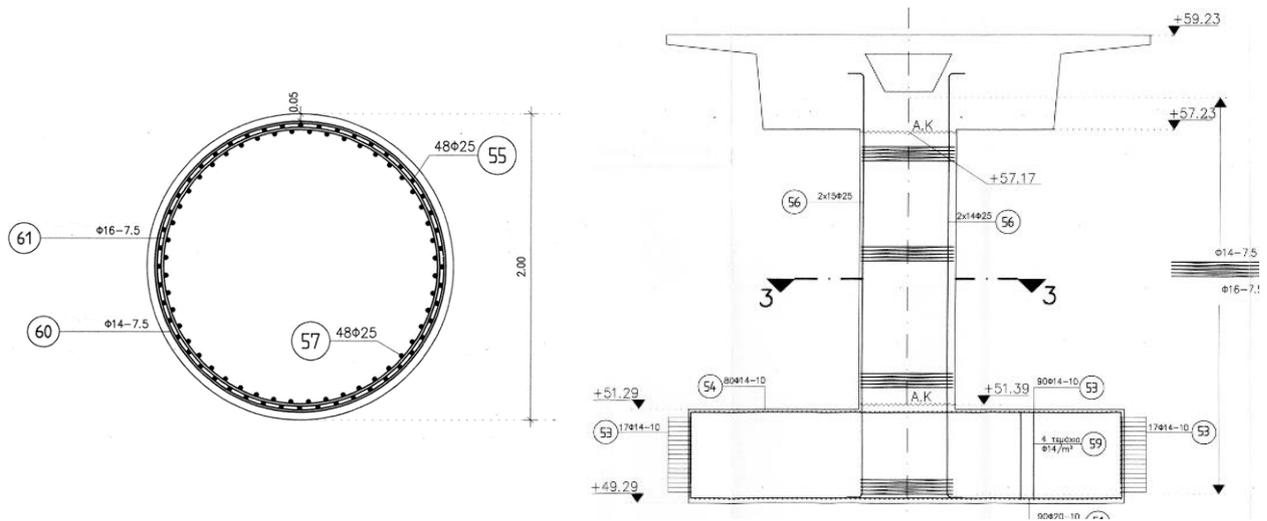
Figure 2. Pier section of T7 bridge (left), section close to the pier

Each seat-type abutment (Fig. 3) consists of backwall, wingwalls and external shear keys. The deck is supported on each abutment through two elastomeric bearings with dimensions (mm) $350 \times 450 \times 136$ and total rubber thickness $t_r = 44$ mm. The total heights of the abutments are 5.63 m and 5.71 m, the height of the backwalls is 2.45 m and their thickness is 0.50 m, while the height of the shear keys is 1.80 m. In the longitudinal direction, a 100 mm joint gap separates the deck from the top of each backwall, while in the transverse direction there is a 150 mm gap between each shear key and the deck.
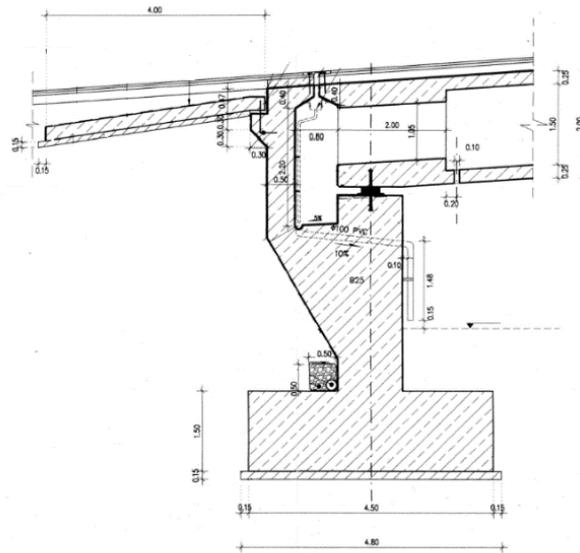
Figure 3. Cross-section at the abutment

The piers and the abutments rest on surface foundation (footings). The dimensions of the pier footings are 9 m $\times$ 8 m $\times$ 2 m and those of the abutment footings are 12 m $\times$ 4.5 m $\times$ 1.5 m. The moderately stiff clay formations of the area ($c_u = 187$ kPa) correspond to soil class C according to Eurocode 8 (CEN, 2005) and due to the absence of measured data, a shear wave velocity $V_s = 300$ m/s (selected as an indicative value within the range of $V_{s,30}$ that corresponds to soil class C in Eurocode 8) and a specific weight $\gamma = 20$ kN/m^3 were assumed for modelling the properties of the soil, resulting in a value of shear modulus at small strains (G_{max}) equal to 183 MPa.

Finite element modelling of the studied bridge

The nonlinear finite element model of the bridge was created using OpenSees (McKenna et al., 2010). The prestressed deck is deemed to remain elastic during the ground motion. The piers are modelled with the *BeamWithHinges* element of OpenSees which is used to model elements with plastic hinges at both ends. The moment-curvature curves required for the definition of each plastic hinge were obtained using the section analysis software *AnySection* (Papanikolaou, 2012). In the software, the confined concrete, the unconfined concrete and the reinforcing steel are represented using the model of Mander et al. as modified by Paulay & Priestley (1992), the nonlinear model of EN1992-1 (CEN, 2004) and the model of Park & Sampson (1972), respectively. The resulting M-φ curves were bilinearised by adopting the criteria of equal energy absorption (equal areas under the initial and the bilinearised M-φ curve) with the ultimate point taken at 15% strength drop.

The elastomeric bearings were modelled as bilinear under horizontal shear and linear elastic under axial load and flexure. The stiffness values for each direction were calculated according to Naeim & Kelly (1999).

Soil-structure interaction at the foundations was taken into account, using equivalent linear soil springs and the closed-form relationships given in Mylonakis et al. (2006) to calculate their secant stiffness for every level of seismic intensity that was used in the analyses. For the estimation of the shear modulus reduction with increasing levels of ground motion, the average values from EN1998-5, Table 4.1 (CEN, 2004) were appropriately interpolated or extrapolated. It is also noted that radiation damping at foundation according to Mylonakis et al. (2006) was considered, but it had minor effect on the response of the studied bridge (e.g., it caused a reduction <0.5% of the maximum displacement at the top of both piers for ground motion scaled to the level of the design earthquake E_d).

The seat-type abutment in the longitudinal direction was modelled according to the simplified approach introduced in Mikes & Kappos (2021), i.e., with a single spring at each end of the deck which represents the nonlinear behaviour of the entire abutment-backfill subsystem resulting from pushover analysis. The abutment-backfill subsystem that was used in the pushover analysis consisted of the backwall, modelled as a *BeamWithHinges* linear element with 5 nonlinear backfill soil springs distributed along its height, and the stem wall (Fig. 4). As shown in Mikes & Kappos (2021) for the abutments of T7, the very large stiffness value of the stem wall results in small displacements even for substantial lateral loads and subsequently to negligible deformation of the backfill soil behind it. As a result, there is no real need to model the soil behind the stem wall. Regarding the backwall, its plastic hinge was modelled in the same way as the pier hinges, while the nonlinear constitutive law of each backfill soil spring was taken to be a hyperbolic curve, following Khalili-Tehrani et al. (2016). For the implementation of the closed-form relationships of Khalili-Tehrani et al. (2016), material properties of highly compacted granular soil were considered for the backfill, as recommended by pertinent codes and guidelines (e.g., Caltrans (2019)). The considered properties of the backfill soil were $\varphi = 40^o$, $\gamma = 20$ kN/m^3, soil strain at 50% of the ultimate stress $\varepsilon_{50} = 0.0035$ m (in line with Shamsabadi et al. (2007) for a similar type of soil), $\nu = 0.35$ and ultimate deformation equal to $0.05H_{bw} = 0.1225$ m, where H_{bw} is the height of the backwall; $0.05H_{bw}$ is an estimation of ultimate deformation of granular backfill soil that adopted in the literature, based on real-scale experiments (Khalili-Tehrani et al., 2016; Shamsabadi et al., 2007).
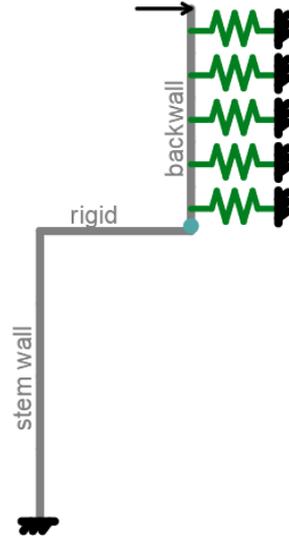
Figure 4. *Longitudinal abutment-backfill model used for the subsystem pushover analysis*

The pushover curve that resulted from the aforementioned procedure was calibrated to the hyperbolic constitutive law of the *HyperbolicGap* material of OpenSees for $d_{gap} = 0$ (Equation 1), proposed by Duncan & Mokwa (2001):

$$F(x) = \frac{x}{\dfrac{1}{K_{max}} + R_f \dfrac{x}{F_{ult}}}$$

(1)

The calibration was achieved with curve fitting via optimisation of K_{max} and R_f terms of Equation 1, implemented in MATLAB (The MathWorks Inc., 2020). The objective function used for the optimisation of K_{max} and R_f was taken to be the sum of squared errors, defined as

$$SSE = \sum \left[F_{pushover}(\delta) - F_{HyperbolicGap}(\delta) \right]^2$$

(2)

The fitted curve is compared with the original resistance curve in Fig. 5. This curve is the backbone curve of the single nonlinear spring at each end of the deck in the case of $d_{gap} = 0$. For $d_{gap} > 0$, a pertinent zero-valued first branch is added to the aforementioned backbone curve. The possibility to add an unloading/reloading branch with stiffness K_{ur} other than the initial K_{init} is an advantage of *HyperbolicGap* compared to other nonlinear constitutive laws with gap provided in OpenSees and other structural analysis software packages, which it is utilised herein. The unloading/reloading stiffness is taken as $K_{ur} = 0.55 \times K_{init}$, based on the suggestion of Cole & Rollins (2006) for backfills consisting of dense gravel.
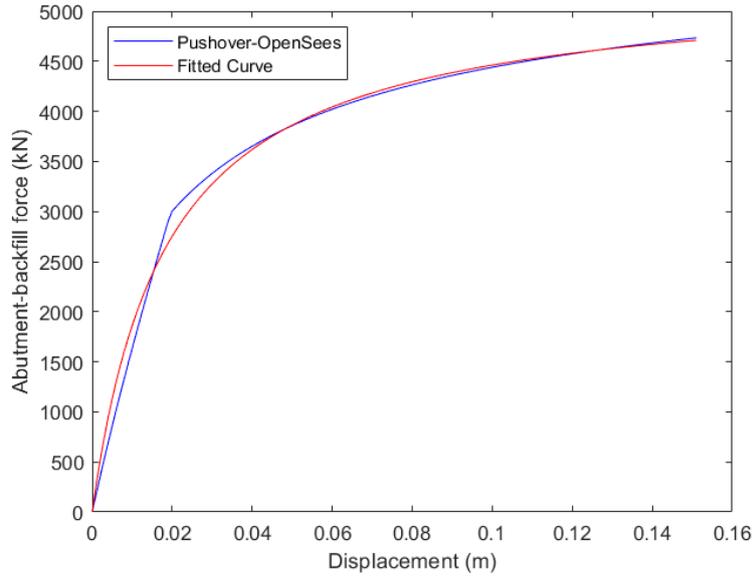
Figure 5. *Fitted curve that was used as the backbone curve of the HyperbolicGap element for $d_{gap} = 0$ compared with the original resistance curve of the T7 abutment-backfill subsystem*

The effect of radiation damping is also taken into account in the longitudinal direction with the use of a viscous damper at each end of the deck, with its dashpot coefficient calculated according to Mylonakis et al. (2006). However, this work refers to surface footings rather than backwalls, therefore an adjustment to take into account the fact that there is no soil above the backwall is made in the same way as in Thomaidis et al. (2020) and Mikes & Kappos (2021) .

In the transverse direction, the shear keys are monolithically connected to the stem wall (no provision of sliding interface), thus the corresponding constitutive law suggested by Silva et al. (2009) is used. In the OpenSees model, a spring with the *ElasticPPGap* constitutive relationship is used to represent each shear key. Since the backbone curve of this constitutive model of OpenSees can have up to two branches and the peak strength point according to Silva et al. (2009) was never reached in the analyses, only the two first two branches (up to the point of peak strength) of the model of Silva et al. (2009) are used (Fig. 6). It is noted that the UCSD tests (Silva et al. 2009) involve a weak stem wall having the same thickness as the shear key, while in the usual case (also in T7) the stem wall is substantially thicker/stronger than the shear key, a case for which no test results are currently available.
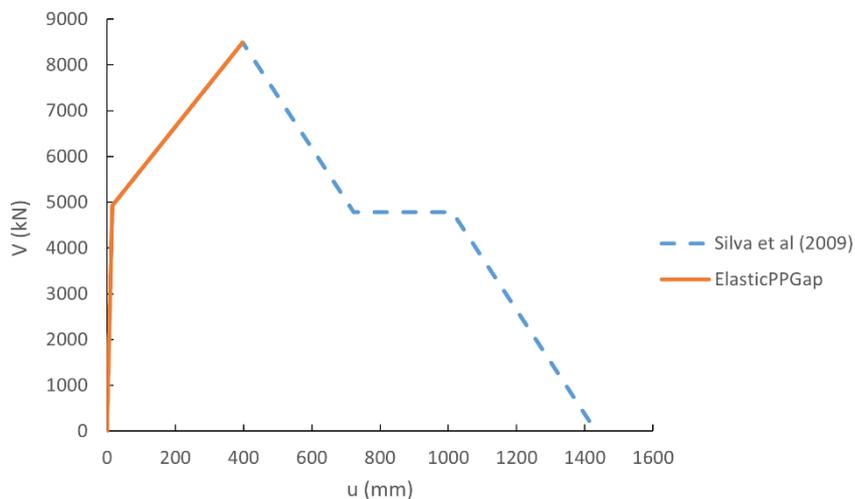
Figure 6. *Backbone curve of the T7 shear key according to Silva et al. (2009) and the part of the curve that was used for the definition of the ElasticPPGap element that represented the shear key*

Nonlinear response history analyses

The nonlinear bridge model described in the previous subsection is subjected to a set of 7 spectrum-compatible artificial accelerograms, scaled to various levels of intensity. The smaller level of intensity is at PGA = 0.08g (50% of the design earthquake E_d) and the largest at PGA = 0.96g (6 times the design earthquake E_d). Soil class C according to Eurocode 8 (CEN, 2005) is considered, but T_D = 4s instead of T_D = 2s is assumed, as a more conservative value for high seismicity regions (Weatherill et al., 2013; Gkatzogias & Kappos, 2019). In both directions, various gap sizes were explored; in the longitudinal direction the gap sizes were d_{gap} = [0 25 50 75 100 125] mm and in the transverse direction they were d_{gap} = [0 50 100 150 200 250] mm. Nonlinear response history analyses (NRHA) are conducted in each direction separately, aiming to obtain a clear view of the effect of the joint gap size and the limit state definition on the assessment of the bridge. So, in each direction, for each level of intensity and each gap size, the average of the responses derived from the analyses with the 7 artificial accelerograms were compared to the limit states defined in Tables 1 and 2, for assessing the performance of the bridge.

RESULTS

Longitudinal direction

The calculated abutment-backfill LS2 thresholds for the studied bridge are $\delta(F_{max}/2)$ = 16 mm according to Bozorgzadeh et al. (2008) and δ = 1% × h_{bw} = 25 mm according to Stefanidou & Kappos (2017). The results for LS2 are shown in Table 3. To better examine the effect of the definition of the abutment-backfill limit state thresholds and their inherent uncertainty, a column with the minimum component safety factor for each limit state threshold is added in Table 3. The minimum component safety factor is defined as the ratio of the average maximum response of the first component that exceeds LS2 over the respective limit state threshold that was adopted. A similar column is also added to Tables 4 and 5.

Table 3. *PGA values at exceedance of LS2 for different definitions of LS thresholds of the abutment-backfill system of T7 bridge and various gap sizes in the longitudinal direction*

d_{gap} (mm)	Abutment-backfill LS2 threshold	LS2 – PGA (g)	LS2 – exceeding component	Minimum component safety factor
0	$\delta(F_{max}/2)$	0.16	Abutment-backfill	1.00
	1% h_{bw}	0.24	Abutment-backfill	0.89
25	$\delta(F_{max}/2)$	0.32	Abutment-backfill	0.78
	1% h_{bw}	0.32	Bearing	0.92
50 – 150	$\delta(F_{max}/2)$	0.32	Bearing	0.86
	1% h_{bw}	0.32	Bearing	0.86

The most important difference is noticed in the case of d_{gap} = 0 (closed gap), where LS2 is marginally exceeded for the set of accelerograms scaled to the design earthquake (E_d, PGA = 0.16 g) under the definition of Bozorgzadeh et al. (2008), while it is clearly exceeded for scaling to 1.5E_d with the less conservative threshold estimation of Stefanidou & Kappos (2017). In both cases, the abutment-backfill component is the first to exceed LS2, indicating that, at least in this case, the option of an entirely closed joint gap in the longitudinal direction is not optimum for earthquake excitation. Obviously, zero gap at the ends would also change the

design of the bridge due to the effect of 'non-seismic' actions (temperature, shrinkage, creep, prestressing), an aspect not addressed further herein. For d_{gap} = 25 mm, both definitions lead to the exceedance of LS2 for $2E_d$. However, the first component to exceed LS2 under the definition of Bozorgzadeh et al. (2008) is the abutment-backfill system with SF = 0.78, meaning that it would also be exceeded if scaling to PGAs between $1.5E_d$ and $2E_d$ were examined. On the other hand, use of the LS2 definition of Stefanidou & Kappos (2017) results in a quite marginal exceedance of LS2 by the bearings first. Besides, it is obvious that differences in the abutment-backfill LS2 threshold definition for joint gap sizes equal to, or larger than, 50 mm are not important, since for such large gap sizes the displacements of the abutment-backfill system decrease and the bearings emerge as the critical component with respect to the "operationality" limit state of the bridge.

The LS4 thresholds considered for the studied bridge were $3 \times \delta(F_{max})$ = 370 mm according to Bozorgzadeh et al. (2008) and 6% h_{bw} = 150 mm according to Stefanidou & Kappos (2017); the broad range delineated by these values is indicative of the uncertainties involved in defining this LS. The only case that LS4 is exceeded is for the maximum level of intensity studied ($6E_d$ or PGA = 0.96 g) and d_{gap} = 0 due to abutment-backfill under the threshold of Stefanidou & Kappos (2017). Referring to the other gap sizes studied, adopting the definition of Stefanidou & Kappos (2017), for gap sizes between 25 mm and 75 mm, the component with the minimum safety factor for intensity equal to $6E_d$ (PGA = 0.96g) is the abutment-backfill and for gap sizes $\geq$ 100 mm, the piers. There is no exceedance of LS4 when the threshold of Bozorgzadeh et al. (2008) is adopted as the piers were the component with the minimum safety factor against LS4 for every considered gap size. It is noted that even for intensity equal to $6E_d$, the safety factor of the piers against LS4, for the largest gap size used in the analyses, is 1.90. The results for LS4 are shown in Table 4. The minimum component safety factor for intensity equal to $6E_d$ (PGA = 0.96g) is shown in this table, since in most cases exceedance of LS4 did not occur for any level of intensity used in the NRHA.

Table 4. PGA values at exceedance of LS4 and minimum component safety factors at PGA = 0.96g for different definitions of LS thresholds of the abutment-backfill system of T7 bridge and various gap sizes in the longitudinal direction

d_{gap} (mm)	Abutment-backfill LS4 threshold	LS4 – PGA (g)	Minimum component safety factor (PGA = 0.96g)
0	$3 \times \delta(F_{max})$	> 0.96	2.12 (Pier)
	6% h_{bw}	0.96	0.98 (Abutment-backfill)
25-75	$3 \times \delta(F_{max})$	> 0.96	2.12 – 2.07 (Pier)
	6% h_{bw}	> 0.96	1.19 – 1.93 (Abutment-backfill)
100-150	$3 \times \delta(F_{max})$	> 0.96	2.02 – 1.90 (Pier)
	6% h_{bw}	> 0.96	2.02 – 1.90 (Pier)

Transverse direction

In the transverse direction, LS4 is not controlled by the abutment-embankment system and the shear keys (the bridge may develop large transverse displacements without safety issues). Therefore, only the threshold values of LS2 are estimated and were found to be $\delta_{y,SK}$ = 15 mm and δ = 0.014 × h_{abut} = 80 mm according to the definitions of Table 2, based on the works of Silva et al. (2009) and Xie et al. (2017), respectively. It should be noted that both definitions are problematic; $\delta_{y,SK}$ seems to be a very conservative estimation of the shear-key LS2 threshold. However, it has to be noted that in the UCSD tests, when shear keys yielded, significant crack opening occurred in the (weak) stem wall. The 1.4% h_{abut} criterion is also hardly relevant for seat-type abutments (the Xie et al. 2017 study addressed integral bridges with diaphragm abutments). There is clearly a lack of a relevant LS definition for the transverse direction of bridges in the literature and the results presented herein should be considered as provisional.

As shown in Table 5, for gaps equal to, or larger than, 50 mm, the definition of the abutment limit state threshold in the transverse direction is not critical for the assessment of the entire bridge, due to the small

displacement values of the shear keys. The "operationality" limit state of the bridge is reached at an intensity equal to E_d and the bearings are the critical component that exceeds the respective threshold first. The contribution of the shear keys is significant in the case of closed gap (as expected), where the exceedance of LS2 occurs for a substantially higher intensity ($2.5E_d$). When the conservative assumption that the LS2 threshold is $\delta_{y,SK}$ is adopted, shear keys are the components that determine the exceedance of the limit state. The assumption that significant separation between abutment and backfill is the LS2 threshold results in exceedance of LS2 at the same level of intensity ($2.5E_d$) but by the piers instead of the abutments.

Table 5. *PGA values at exceedance of LS2 for different definitions of LS thresholds of the abutment-embankment system of T7 bridge and various gap sizes in the transverse direction*

d_{gap} (mm)	Abutment-embankment LS2 threshold	LS2 – PGA (g)	LS2 – exceeding component	Minimum component safety factor
0	$\delta_{y,SK}$	0.40	Abutment-backfill	0.77
	1.4% h_{abut}	0.40	Pier	0.88
50-250	$\delta_{y,SK}$	0.16	Bearing	0.75
	1.4% h_{abut}	0.16	Bearing	0.75

CONCLUSIONS

This paper explored for the first time the significance of considering limit states related to the abutment-backfill system on the design or assessment of bridges and evaluated the effect of different definitions of the abutment-backfill limit states of 'operationality' (LS2) and 'collapse prevention – life safety' (LS4). This was pursued by taking into account the end gap size which is critical for the mobilization of the abutment-backfill system. Ranges of the LS thresholds were considered and applied for the assessment of the seismic performance of an existing concrete bridge constructed according to modern seismic provisions.

In the *longitudinal* direction of the bridge, the definition of the abutment-backfill state affected, to some extent, both LS2 and LS4 of the bridge. Although the range of the LS2 threshold values found in the literature was the smallest among the examined limit states, the two values that were adopted led to different results in the assessment of the bridge in the cases that small or closed joint gaps were used. This can be attributed to the fact that small gap sizes result in considerable abutment-backfill displacements even for relatively low earthquake intensities due to the deck-abutment collision. Much larger uncertainty was observed in the definition of the LS4 abutment-backfill threshold in the literature since the maximum value mentioned was almost 2.5 times the minimum one. This large difference underlines the need for more meticulous work towards a more accurate identification of the abutment-backfill limit state which is critical for the stability of the bridge and for the life safety of the users during an earthquake, based on both geotechnical and structural criteria. The conservative definition of LS4 was found to be critical in the case of closed end gaps; however, it must be noted that the studied bridge was clearly overdesigned since it withstood without failure ground motions equal to even $6E_d$ in all NRHA. As a result, studies of more economically designed bridges may be useful in drawing important conclusions regarding the significance of the large uncertainty in the definition of the abutment-backfill LS4 thresholds in the longitudinal directions.

Regarding the *transverse* direction, in the case of closed transverse gap not only was the shear key the first component that exceeded LS2, but also its contribution enhanced the behaviour of the bridge notably by increasing the LS2 PGA value from 0.16g to 0.40g. It is clear, though, that the information on LS thresholds in the transverse direction available in the literature is far from sufficient or satisfactory, particularly for the usual case of seat-type abutments. This is attributed to the lack of experimental work focused on the response of abutments in this direction, while analytical studies (and response measurements in real bridges) involve primarily integral bridges. It is pointed out that the often adopted relationships for shear keys derived on the basis of the UCSD experiments (Silva et al. 2009), lead to unreliable results in the usual case that the shear

keys (rather than the stem wall) are the elements where damage will concentrate. The findings of the present paper underscore the importance of developing more appropriate limit state criteria for the transverse direction covering a broader range of abutment and shear key typologies.

ACKNOWLEDGEMENT

REFERENCES

Bozorgzadeh, A., Ashford, S. A., Restrepo, J. I., & Nimityongskul, N. (2008). Experimental and Analytical Investigation on Stiffness and Ultimate Capacity of Bridge Abutments,(59). *SSRP*, *7*, 12.

Caltrans (California Department of Transportation). (2019). *Seismic design criteria version 2.0*.

Cardone, D. (2014). Displacement limits and performance displacement profiles in support of direct displacement-based seismic assessment of bridges. *Earthquake Engineering & Structural Dynamics*, *43*(8), 1239–1263.

CEN. (2004). Eurocode 8: Design of structures for earthquake resistance Part 5: Foundations, retaining structures and geotechnical aspects. *Brussels, European Committee for Standardization*.

CEN. (2005). Eurocode 8: Design of structures for earthquake resistance-part 1: general rules, seismic actions and rules for buildings. *Brussels: European Committee for Standardization*.

CEN (2004). (2004). Eurocode 2: Design of concrete structures—Part 1-1: General rules and rules for buildings. *EN 1992-1-1. Brussels, European Committee for Standardization*.

CEN (2005). (2005). Eurocode 8: Design of Structures for Earthquake Resistance–Part 2: Bridges. *Brussels, European Committee for Standardization*.

Cole, R. T., & Rollins, K. M. (2006). Passive earth pressure mobilization during cyclic loading. *Journal of Geotechnical and Geoenvironmental Engineering*, *132*(9), 1154–1164.

Duncan, J. M., & Mokwa, R. L. (2001). Passive earth pressures: theories and tests. *Journal of Geotechnical and Geoenvironmental Engineering*, *127*(3), 248–257.

Gkatzogias, K. I., & Kappos, A. J. (2019). Direct estimation of seismic response in reduced-degree-of-freedom isolation and energy dissipation systems. *Earthquake Engineering and Structural Dynamics*, *48*(10), 1112–1133.

Khalili-Tehrani, P., Shamsabadi, A., Stewart, J. P., & Taciroglu, E. (2016). Backbone curves with physical parameters for passive lateral response of homogeneous abutment backfills. *Bulletin of Earthquake Engineering*, *14*(11), 3003–3023.

Kim, S.-H., & Feng, M. Q. (2003). Fragility analysis of bridges under ground motion with spatial variation. *International Journal of Non-Linear Mechanics*, *38*(5), 705–721.

LaFave, J., Fahnestock, L., Foutch, D. A., Steelman, J., Revell, J., Filipov, E., & Hajjar, J. F. (2013). *Experimental investigation of the seismic response of bridge bearings*.

McKenna, F., Scott, M. H., & Fenves, G. L. (2010). Nonlinear Finite-Element Analysis Software Architecture Using Object Composition. *Journal of Computing in Civil Engineering*, *24*(1), 95–107. https://doi.org/10.1061/(asce)cp.1943-5487.0000002

Mikes, I. G., & Kappos, A. J. (2021). Simple and complex modelling of seat-type abutment-backfill systems. *Proceedings of the International Conference on Computational Methods in Structural Dynamics and Earthquake Engineering*, *2021*, 5266–5282.

Moulton, L. K. (1986). *Tolerable movement criteria for highway bridges*. United States. Federal Highway Administration.

Mylonakis, G., Nikolaou, S., & Gazetas, G. (2006). Footings under seismic loading: Analysis and design issues with emphasis on bridge foundations. *Soil Dynamics and Earthquake Engineering*, *26*(9), 824–853.

Naeim, F., & Kelly, J. M. (1999). *Design of seismic isolated structures: from theory to practice*. John Wiley & Sons.

Papanikolaou, V. K. (2012). Analysis of arbitrary composite sections in biaxial bending and axial load. *Computers & Structures*, *98*, 33–54.

Park, R., & Sampson, R. A. (1972). Ductility of reinforced concrete column sections in seismic design. *Journal Proceedings*, *69*(9), 543–555.

Paulay, T., & Priestley, M. J. N. (1992). *Seismic design of reinforced concrete and masonry buildings*. Wiley New York.

Shamsabadi, A., Rollins, K. M., & Kapuskar, M. (2007). Nonlinear soil–abutment–bridge structure interaction for seismic performance-based design. *Journal of Geotechnical and Geoenvironmental Engineering*, *133*(6), 707–720.

Silva, P. F., Megally, S., & Seible, F. (2009). Seismic performance of sacrificial exterior shear keys in bridge abutments. *Earthquake Spectra*, *25*(3), 643–664.

Stefanidou, S. P., & Kappos, A. J. (2017). Methodology for the development of bridge-specific fragility curves. *Earthquake Engineering & Structural Dynamics*, *46*(1), 73–93.

Stefanidou, S. P., Paraskevopoulos, E. A., Papanikolaou, V. K., & Kappos, A. J. (2022). An online platform for bridge-specific fragility analysis of as-built and retrofitted bridges. *Bulletin of Earthquake Engineering*, 1–21.

The MathWorks Inc. (2020). *MATLAB v.9.8.0 1380330 (R2020a)* (9.8.0 1380330 (R2020a)). The Mathworks Inc.

Thomaidis, I. M., Kappos, A. J., & Camara, A. (2020). Dynamics and seismic performance of rocking bridges accounting for the abutment-backfill contribution. *Earthquake Engineering & Structural Dynamics*, *49*(12), 1161–1179.

Weatherill, G., Crowley, H., & Danciu, L. (2013). Preliminary reference Euro-Mediterranean seismic hazard zonation. In *Zürich, CH: Swiss Seismological Service. Seismic Hazard Harmonization in Europe (SHARE)*.

Xie, Y., Huo, Y., & Zhang, J. (2017). Development and validation of p-y modeling approach for seismic response predictions of highway bridges. *Earthquake Engineering & Structural Dynamics*, *46*(4), 585–604.